

Neuromorphometric characterization with shape functionals

Marconi Soares Barbosa* and Luciano da Fontoura Costa[†]

*Cybernetic Vision Research Group, GII-IFSC. Universidade de São Paulo,
São Carlos, SP, Caixa Postal 369, 13560-970, Brasil*

Esmerindo de Sousa Bernardes[‡]

*Departamento de Física e Ciência dos Materiais. Universidade de São Paulo,
São Carlos, SP, Caixa Postal 369, 13560-970, Brasil*

(Dated: November 11, 2018)

Abstract

This work presents a procedure to extract morphological information from neuronal cells based on the variation of shape functionals as the cell geometry undergoes a dilation through a wide interval of spatial scales. The targeted shapes are alpha and beta cat retinal ganglion cells which are characterized by different ranges of dendritic field diameter. Image functionals are expected to act as descriptors of the shape, gathering relevant geometric and topological features of the complex cell form. We present a comparative study of classification performance of additive shape descriptors, namely Minkowski functionals, and the non-additive multi scale fractal. We found that the new measures perform efficiently the task of identifying the two main classes, α and β , based solely on scale invariant information, while also providing intraclass morphological assessment.

PACS numbers: 87.80.Pa, 87.19.La

*marconi@if.sc.usp.br

†luciano@if.sc.usp.br

‡sousa@if.sc.usp.br

I. INTRODUCTION

Many natural phenomena are defined or influenced by the geometrical properties of the involved elements, and vice-versa. Examples of such a shape-function relationship include the chemical properties of proteins, the aerodynamic efficiency of wings, and the oxygen exchanges through elaborated bronchic structures. The close relationship between geometry and function provides strong motivation for the geometrical analysis of natural objects. Yet, the state-of-the-art of geometrical characterization, an area sometimes called morphometry or morphology, remains in a relatively incipient stage where several competing, and often divergent, approaches coexist. While powerful methods have been used in physics to express relevant geometrical properties, often including differential measurements such as curvature, the situation remains particularly challenging in biology.

The relationship between neuronal shape and function has attracted increasing attention due to its far reaching implications for basic neuroscience and for medical applications. Neuron morphology has the special characteristic, that it evolves during the developmental stage of the cell, being influenced by its molecular environment and the history of synaptic activity [1]. The mature neuronal shape, together with its membrane electrical properties, determine the electric conductance of the cell [2] and account for part of its electrophysiological characteristics such as firing patterns and computational abilities [3, 4, 5, 6]. Software packages, such as NEURON, are available for modelling neuronal activity with basis on cable theory [7] which can be useful for analysis of real or virtual neurons [8, 9, 10]. At the same time, neuronal shape can vary for different tissues, depending on a number of extracellular factors [1, 11]. Ultimately, it determines the patterns of connectivity and, consequently, the overall network computational abilities. On the application side, tasks such as automated morphological characterization of neuronal shape and the diagnosis of abnormalities, deserve further investigation.

While the use of morphological tools was severely constrained until recently by the cost of the relatively sophisticated systems needed to process images and geometry, the continuing advances in computer software and hardware have paved the way for an ever widening range of possible applications. Consequently, more effective morphological concepts and methods have been developed and reported in the literature, including the use of differential geometry concepts such as multi-scale curvature and bending energy [12, 13, 14], methods

from mathematical morphology such as skeletonization [15, 16], as well as the recently reported framework known as Integral-Geometry Morphological Image Analysis (MIA) [17, 18, 19]. The latter approach involves the use of additive shape functionals, i.e. mappings that take shapes to single scalar values, in terms of a parameter usually related to the spatial scale or time. As far as neuroscience is concerned, the contour of a neuronal cell has been shown to possess a fractal structure [20] and its multiscale fractal dimension been used to characterize different morphological classes of neuronal cells [21].

Primarily motivated by the possibility of applying the methodology proposed in [17, 18] as a novel and potentially useful tool for addressing the problem of neuronal shape characterization and classification, the present work also provides an assessment of those measures considering a database of real biological data, namely camera lucida images of cat ganglion neuronal cells. In order to provide a comparative reference, the multi-scale fractal dimension [21], itself a shape functional, is also considered as a measure for shape characterization.

Integral geometry provides an adequate mathematical framework for morphological image analysis, having a core of useful theorems and formulae that in some cases leads to analytical results for averages of image functionals [19] while also being quite efficient to implement computationally [18]. Here, the class of functionals involved are restricted to additive, motion invariant and continuous, called Minkowski functionals. These functionals are related to usual geometric quantities, for instance, in the Euclidean plane, to area, perimeter and connectivity or the Euler number, which expresses the number of holes in a connected pattern such as the image of a neuronal cell.

In order to describe geometrically one object, a set of measures (functionals) is taken and the behaviour of these measures is monitored, as some control parameter is varied. In this work we compute additive functionals in the plane as the contour of a neuronal cell image is inflated by a parallel set dilation of radius r , the control parameter. The non-additive multi scale fractal dimension is derived from one of those computed additive functionals, at each radius of dilation, giving important [22] complementary information.

This article starts by presenting the adopted methodology, the considered shape functionals, and the statistical procedure for cell identification. The results, which are presented subsequently, clearly indicate that the new measures are efficient for distinguishing morphologically the two functional classes alpha and beta as well as revealing a strong morphological

coherence in one of the classes.

II. METHODOLOGY

A. Additive shape functionals

The morphological characterization in Euclidean plane by means of shape functionals explores simple properties of convex sets. For these basic geometric objects, such as triangle or an ellipse, we may evaluate a change in area while the object undergoes a morphological dilation with the knowledge of its initial geometry. For example the change in area of a convex body K , after a parallel set dilation using a 2D ball of radius r , can be expressed as

$$A(K_r) = A(K) + U(K)r + \pi r^2, \quad (1)$$

where $A(K)$ and $U(K)$ stand for the initial area and perimeter of the object K and r is the dilation parameter. The process of taking parallel sets generalises naturally to higher dimensions, while the change in hyper volume preserves the general form (1) and is given by the Steiner formula

$$v^d(K_r) = \sum_{\nu=0}^d \binom{d}{\nu} W_{\nu}^{(d)}(K) r^{\nu}, \quad (2)$$

where the coefficients $W_{\nu}^{(d)}$ are referred to as *quermassintegrals* or Minkowski functionals, [17]. These functionals, as a generalisation of known geometric quantities, are additive, motion invariant and continuous. Moreover, a Theorem by Hadwiger [17, 19] states that these functionals form a complete set of measures, with the above properties, on the set of convex bodies

$$\phi(K) = \sum_{j=0}^d c_j W_j^{(d)}(K). \quad (3)$$

Notwithstanding, the change of any, additive, motion invariant and continuous functional can be expressed, using a generalised Steiner formula [19, 23], in terms of the initial geometric information

$$\phi(K_r) = \sum_{j=0}^d \sum_{k=0}^{d-j} c_j \binom{d-j}{k} W_{k+j}^{(d)}(K) r^k. \quad (4)$$

The notion of connectivity number or Euler characteristic χ is central in establishing the aforementioned properties of Minkowski functionals. The usual definition of the connectivity

from algebraic topology in two dimensions is the difference between the number of connected n_c components and the number of holes n_h ,

$$\chi(K) = n_c - n_h, \quad (5)$$

while in three dimensions distinction should be made between two kind of holes namely cavities n_{hc} and handles(tunnels) n_{hh}

$$\chi(K) = n_c - n_{hh} + n_{hc}. \quad (6)$$

Integral Geometry provides an equivalent definition for connectivity number of a convex set K which is given by

$$\chi(K) = \begin{cases} 1 & K \neq \emptyset \\ 0 & K = \emptyset. \end{cases} \quad (7)$$

Of great importance is its property of additivity

$$\begin{aligned} \chi(A) = \chi(\cup_{i=1}^l K_i) &= \sum_i \chi(K_i) - \sum_{i < j} \chi(K_i \cap K_j) + \dots \\ &\dots + (-1)^{l+1} \chi(K_1 \cap \dots \cap K_l). \end{aligned} \quad (8)$$

Additivity and motion invariance is inherited by the Minkowski functionals as they are related to the connectivity number by the formulae

$$\begin{aligned} W_\nu^{(d)}(A) &= \int_{\mathcal{G}} \chi(A \cap E_\nu) d\mu E_\nu \quad \nu = 0, \dots, d-1 \\ W_d^{(d)}(A) &= \omega_d \chi(A), \quad \omega_d = \pi^{d/2} / \Gamma(1 + d/2). \end{aligned} \quad (9)$$

In the above expression E_ν stands for an ν -dimensional plane in \mathbb{R}^d . The integral is to be taken for all positions, induced by isometries \mathcal{G} , of E_ν weighted by $d\mu(E_\nu)$, the kinematical density which is in turn related to the Haar measure on the group of motions \mathcal{G} , see [17, 19, 23].

To sum up, the Minkowski functionals $W_\nu^{(d)}(A)$, as a generalisation of the usual procedure for volume determination, counts the number of possible intersection of a ν -dimensional plane with the domain A .

If one is to take advantage of the above additivity property all intersection in (8) must be taken into account. When working on a lattice, there is a more expedient route, exploring

m	\check{N}_m	$W_0^{(2)} = A(\check{N}_m)$	$W_1^{(2)} = \frac{1}{2}U(\check{N}_m)$	$W_2^{(2)} = \pi\chi(\check{N}_m)$
0	\check{P}	0	0	π
1	\check{L}	0	a	$-\pi$
2	\check{Q}	a^2	$-2a$	π

TABLE I: Minkowski functionals of elementary open bodies which compose a pixel K .

the discrete nature of the images and the additivity of the Minkowski functionals, which consists of a decomposition of the 2D body A into a disjoint collection of interior bodies, open edges and vertices. Following the usual nomenclature we denote the interior of a set A by $\check{A} = A/\partial A$. For an open interior of a n -dimensional body embedded in a d -dimensional Euclidean space there is the following expression for the Minkowski functionals, [17],

$$W_\nu^{(d)}(\check{A}) = (-1)^{d+n+\nu}W_\nu^{(d)}(A), \quad \nu = 0, \dots, d. \quad (10)$$

We may then apply additivity and the lack of connectivity of open sets on the lattice to determine the functionals for the body as a whole

$$W_\nu^{(d)}(\mathcal{P}) = \sum_m W_\nu^{(d)}(\check{N}_m)n_m(\mathcal{P}), \quad \nu = 0, \dots, d. \quad (11)$$

Where $n_m(\mathcal{P})$ stands for the number of building elements of each type m occurring in the pattern \mathcal{P} . For a two dimensional space which is our interest for the present neuron images, we display in Table I the value of Minkowski functionals for the building elements on a square lattice of pixels and their direct relation to familiar geometric quantities on the plane. Using the information presented in Table I and equation (11) we have

$$A(\mathcal{P}) = n_2, \quad U(\mathcal{P}) = -4n_2 + 2n_1, \quad \chi(\mathcal{P}) = n_2 - n_1 + n_0. \quad (12)$$

So the procedure of calculating Minkowski functionals of a pattern \mathcal{P} has been reduced to the proper counting of the number of elementary bodies of each type that compose a pixel (squares, edges and vertices) involved in the make up of \mathcal{P} .

In section III we describe typical results for the evaluation of the above presented additive functionals using an actual neuron image. The procedure involves the implementation of, first an algorithm for the proper parallel set dilation throughout all permitted radius on the square lattice and, second, of an algorithm for the calculation of Minkowski functionals

by counting disjoint building elements based on the formulae (12). An efficient routine for undertaking the latter is described in detail in [17, 18].

B. Multi scale fractal dimension

As an example of a related non-additive functional, we add to the previous measures the multi scale fractal, an approach which has been applied successfully to neuromorphometry [22]. The notion of multi-scale fractal dimension refers to a quantitative characterization of complexity and the degree of self-similarity at distinct spatial scales, see [21, 22]. Intuitively, the fractal dimension indicates how much the curve extends itself throughout the space. As a consequence, more intricate curves will cover the surround space more effectively and will display a higher fractal dimension. This quantity is calculated via the derivative of the logarithm of the changing interior area as the neuron cell image undergoes a dilation. As such it is immediately derivable from the first additive functional (Area) in a pixel based approach as opposed to a curvature approach, see [21].

C. Implementation

We have conducted the evaluation of the functionals described above on a 800MHz ordinary personal computer running Linux. Both the algorithm for exact dilations on the square lattice, according to [24] and the pixel based algorithm for the estimation of the Minkowski functionals [17] was implemented in SCILAB-2.6. It took approximately 40s to calculate the functionals for each dilation radius.

III. RESULTS

We start by describing a measure that is perhaps the simplest one but which holds important information not only on its own, but through relation with the multi scalar fractal dimension described in section II B. In Figure 3 we show the typical monotonically increasing curve of the interior area of a neuron cell as its contour is inflated by a parallel set procedure. To capture the gross structure of this measure we calculate the area under the curve, sum^a , and in a size independent manner, the radius $R_{\frac{1}{2}}^a$ at which the area below

this curve reaches half of its value at the end of dilation. The fine structure is given by its standard deviation, std^a .

In Figure 4 we show a typical curve of the perimeter of the evolving frontier of the neuron cell as the contour is inflated by a parallel set procedure. It is important to observe that this measure is affected by errors introduced by the discrete nature of the lattice of pixels and the low resolution of the original image, which becomes more acute in beta cells because of their reduced size. Nonetheless, this effect tends to be less important after the tenth radii or so. To capture the gross structure of this measure, we calculate the area under the curve sum^p and the size independent radius $R_{\frac{1}{2}}^p$ at which the area below this curve reaches half of its overall value. The fine structure is given simply by the standard deviation of the data, std^p .

In contrast to the preceding measure the connectivity or the Euler number of the neuron shape as it undergoes the dilation processes is independent of the resolution of the image. It is a measure restricted to the topology of the shape counting essentially the number of holes at each radius of dilation no matter the holes are perfectly round or not. The alterations of connectivity are subtle from step to step, which is reflected by the complex distribution of cusps in Figure 5. The vast amplitude of scale for which there is an abrupt change of connectivity is a measure of complexity of this type of cell. Figure 6 shows the particular behaviour of the connectivity, for samples from the two classes, as the cell shape undergoes a dilation. We take the gross information of this measure by extracting the area under the interpolated curve, $\text{sum}_{\text{interp}}$, and a monotonicity index given by

$$i_s = \frac{s}{s + d + p}, \quad (13)$$

where s , d and p counts respectively the number of times that the curve increase, decrease or reach a plateau. This index characterizes a perfect monotonically increasing curve when its value is 1 and reaching its minimum value for a curve of high variability. This measure is designed specially to explore the multi-scale nature of the neuronal complexity. The finer structure is captured solely by the standard deviation std_{diff} of the difference between the interpolated curve and the original data.

As a measure of complexity, the multi-scale fractal dimension has been experimentally found to be related to the connectivity of a shape. Although this relationship is not straightforward, there might be a correlation between these measures as commented bellow. For

this image functional, we evaluate the maximum fractal dimension, the mean fractality and the standard deviation, respectively \max , mean and std^f . A typical curve for the multi scale dimension is shown in Figure 7 for the same neuron appearing in Figure 1.

Among all the considered measurements, we found a good separation of alpha and beta type cells for the feature space defined by the perimeter half integral radius, $R_{\frac{1}{2}}^p$, and the standard deviation for the fine structure of connectivity, std_{diff} . Figure 8 shows the obtained alpha and beta clustering with both class exhibiting similar dispersion. Another good result for morphological characterization was obtained for the connectivity or the Euler number of the cell shape. A feature space involving the index of monotonicity and the integral of the interpolated connectivity curve is presented in Figure 9. More efficient than the former in separating the two classes, these measures produce a well localised clustering of beta cells characterising its geometrical intricacies. This result suggests that alpha class is indeed a more homogeneous category while the beta class may have a morphological subclass structure.

Table II shows the correlation coefficients for the twelve measurements considered in this work. Of special interest is the correlation between fractality and connectivity, measures that have experimentally been found to represent complementary but not redundant measures of complexity. Figure 10 shows a combination of two measures to form a feature space which in this case shows a poor separation of classes which is in accordance with the high anti-correlation of the involved measures presented in Table II. Unusually high correlation appears between some measures notably as occurring between area and perimeter, suggesting a specific tendency that seems to be particular to the type of data (neurons) and not a general rule.

IV. CONCLUSIONS

The use of additive shape functionals has been recently considered for the characterization of the geometrical properties of several physical objects [17, 19]. The current article explored the use of a representative set of such functionals, namely the area, perimeter and connectivity, for the characterization of neural shapes represented in terms of a whole set of parallel expansions. The multi scale fractal dimension, a non-additive shape functional, was also considered as a standard for comparison.

All the adopted shape functionals consist of functions of the dilating radius of each parallel body. For the sake of efficiency, the following compact subset of global features was selected: the area under the functionals, the value of radius where the area reaches its half-value, the standard deviation of the functionals, as well as a novel measurement expressing the monotonicity of the functionals and the decomposition of the connectivity functional in terms of a low and high variation signals.

All two-by-two combinations of these measures were investigated visually in order to identify the combinations of features leading to more pronounced separations between the two classes of considered neural cells, namely cat retinal ganglion cells of type alpha and beta. The coefficients of correlation of each pair of measures were also estimated and analysed, indicating decorrelation between several of the considered features. The obtained results confirmed a differentiated potential of each measurement for neural cell clustering, with the features derived from the connectivity functional accounting for the best separation between classes. However, further investigations and comparison to more established and recent methods (such as in [25]) based explicitly on dendritic morphology will be necessary to reveal the best realization of the novel methodology proposed in this article. The biological implications of such results are that the two type of cells differ in the distribution of holes (defined by the respective dendritic arborizations) for different spatial scales. The obtained clusters indicated that the alpha cells exhibit less uniform geometrical properties than the beta, suggesting the existence of morphological subclasses.

Acknowledgments

The authors are grateful to FAPESP (processes 02/02504-01, 99/12765-2 and 96/05497-3) and to CNPQ (process 301422/92-3) for financial support.

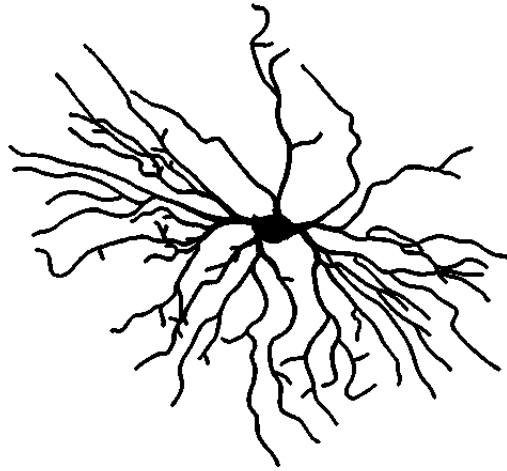


FIG. 1: Initial neuron image. Reprinted with permission from B.B. Boycott and H. Wässle. *J. Physiol*(1974) 240 page 402.

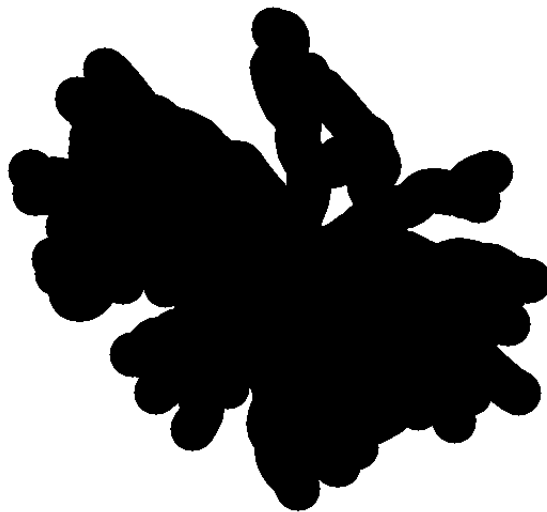


FIG. 2: The same neuron image after the parallel set dilation.

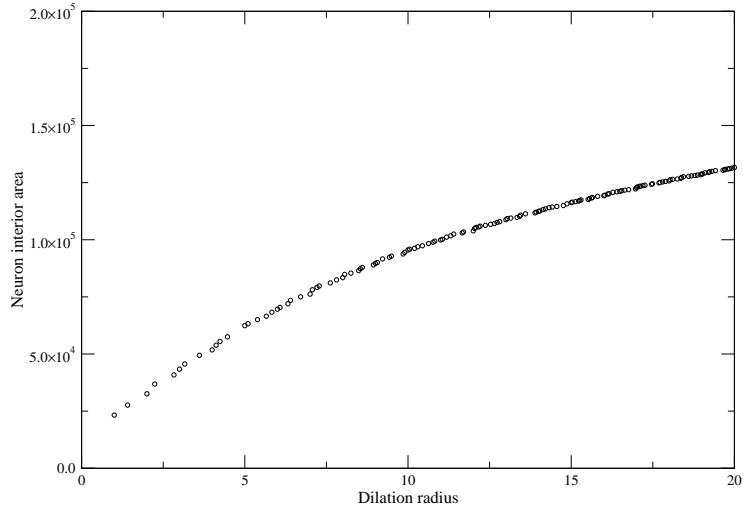


FIG. 3: Area (in pixels) as a function of the scale radius (in pixels) for a typical alpha neuronal cell given in Figure 1. Subtle information in this graphic is revealed only through the multi-scale fractal dimension.

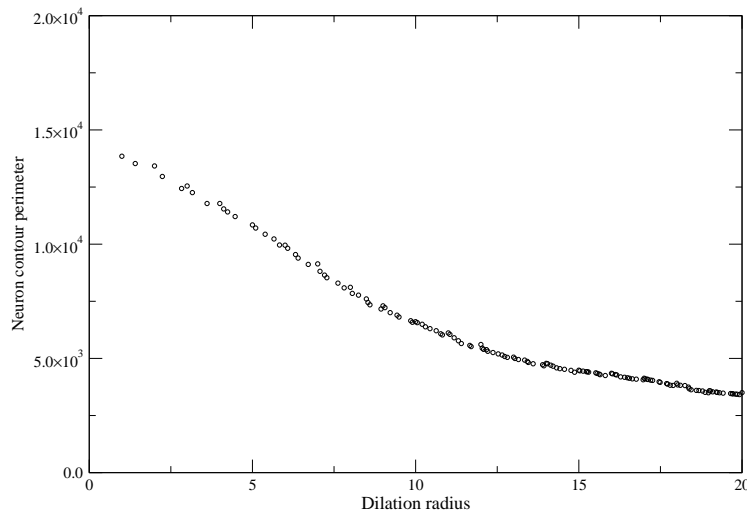


FIG. 4: Perimeter (in pixels) as a function of the scale radius (in pixels) for the alpha neuronal cell of Figure 1. Note the expected initial decline and a visible fine structure associated with the disappearing and less frequently appearing holes.

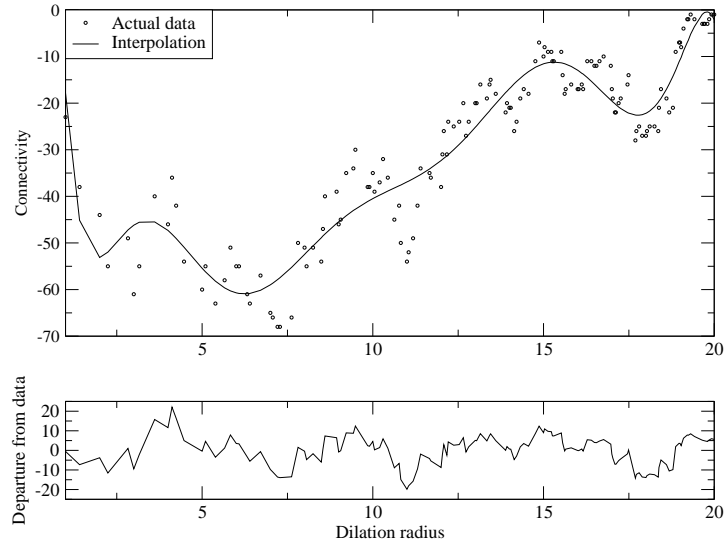


FIG. 5: Connectivity and the difference between data and interpolation for the typical alpha neuronal cell, Figure 1, as a function of parallel set dilation radius (in pixels).

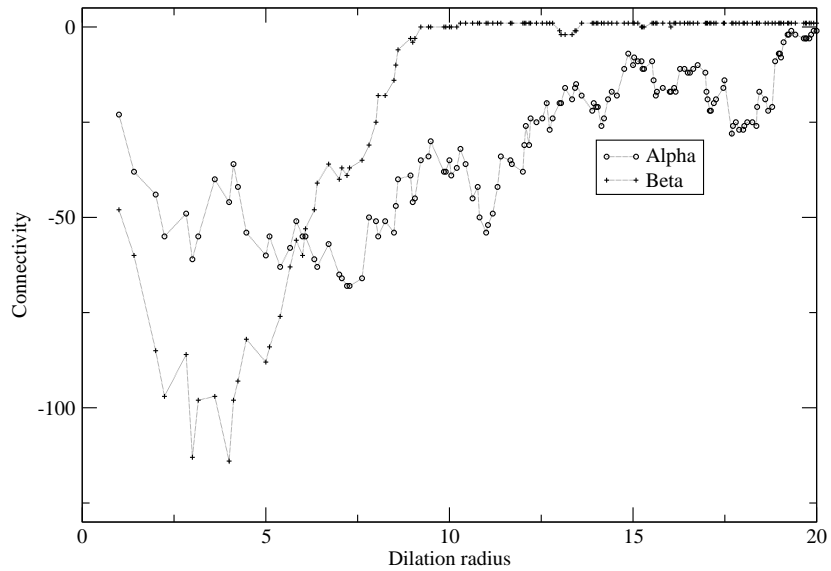


FIG. 6: Comparison between the connectivity of typical alpha and beta cells showing a different range (in pixels) of complexity for the two class of neurons.

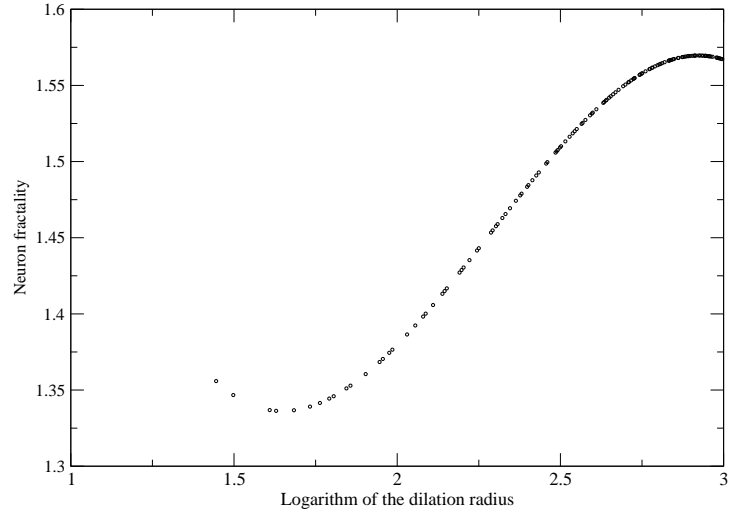


FIG. 7: Multi scale fractality of a neuronal type alpha cell. This attribute is obtained from the area functional and shows the fine structure that is not revealed by that functional alone. Dilation radius in pixels.

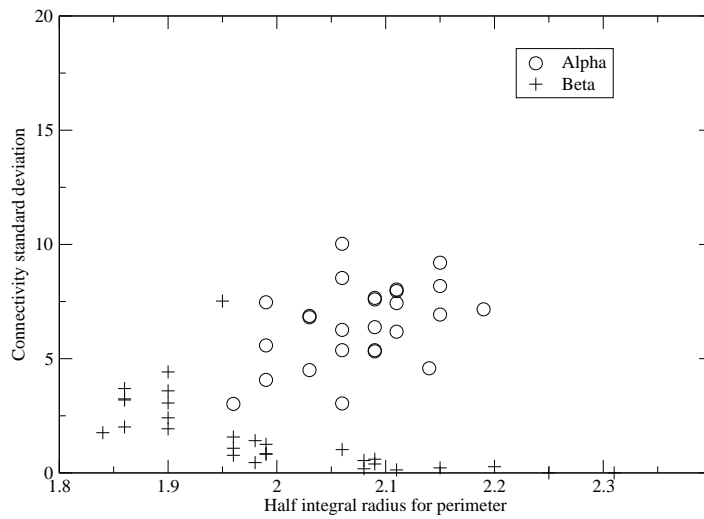


FIG. 8: Clustering of alpha and beta cells based on $R_{1/2}^P$ (in pixels) and connectivity measures.

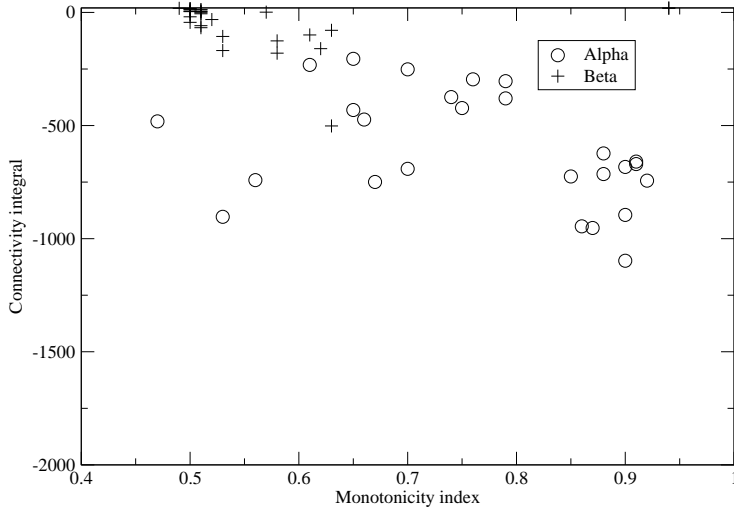


FIG. 9: The feature space based on the index of monotonicity and the integral of the connectivity (interpolated) curve, for both alpha and beta cells showing a strong clustering of the beta neuron class and a much dispersed alpha class.

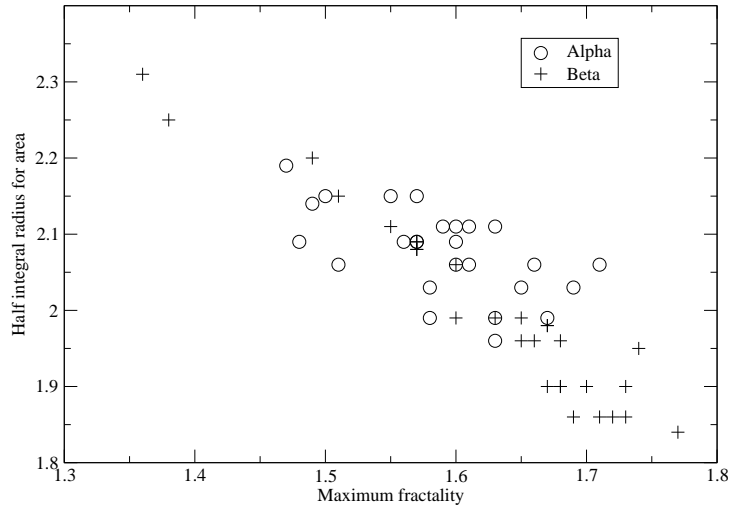


FIG. 10: A not decisive feature space: related measures with high (anti-)correlation. Half integral radius in pixels.

	Area			Perimeter			Connectivity			Fractality		
	std^a	sum^a	$R_{1/2}^a$	std^p	sum^p	$R_{1/2}^p$	std_{diff}	$\text{sum}_{\text{interp}}$	i_s	std^f	max	mean
std^a	1											
sum^a	0.96	1										
$R_{1/2}^a$	0.51	0.41	1									
std^p	0.86	0.96	0.33	1								
sum^p	0.97	0.99	0.45	0.94	1							
$R_{1/2}^p$	0.13	0.01	0.78	-0.05	0.03	1						
std_{diff}	0.78	0.88	0.15	0.90	0.87	-0.27	1					
$\text{sum}_{\text{interp}}$	-0.79	-0.92	-0.22	-0.98	-0.90	0.17	-0.92	1				
i_s	0.33	0.44	0.34	0.52	0.44	-0.02	0.43	-0.57	1			
std^f	-0.24	-0.27	0.16	-0.19	-0.27	0.58	-0.40	0.27	-0.34	1		
max	-0.34	-0.18	-0.86	-0.01	-0.23	-0.65	0.05	-0.07	-0.22	0.10	1	
mean	0.14	0.30	-0.63	0.39	0.26	-0.88	0.55	-0.49	0.22	-0.64	0.63	1

TABLE II: Correlation coefficients for the set of the measures extracted from Area, Perimeter, Connectivity and Fractality: Standard deviations ($\text{std}^{a,p,f}, \text{std}_{\text{diff}}$), Integrals ($\text{sum}^{a,p}, \text{sum}_{\text{interp}}$), Half radii ($R_{1/2}^{a,p}$), the monotonicity index (i_s), mean value (mean) and max value (max). Bold face for absolute values of correlation above 0.5.

-
- [1] K. L. Whitford, P. Dijkhuizen, F. Polleux, and A. Ghosh, *Annual Review of Neuroscience* **25**, 127 (2002).
- [2] C. Koch and I. Segev, *Nature Neuroscience suppl.* **3**, 1171 (2000).
- [3] A. van Ooyen, J. Duijnhouwer, M. W. H. Remme, and J. van Pelt, *Network: Comput. Neural Syst.* **13**, 311 (2002).
- [4] Y. Fukuda, C. F. Hsiao, M. Watanabe, and H. Ito, *J. Neurophysiol.* **52**, 999 (1984).
- [5] H. Wässle, B. B. Boycott, and R. B. Illing, *Phil. Trans. R. Soc.* **212**, 177 (1981).
- [6] H. G. Krapp, B. Hengstenberg, and R. Hengstenberg, *J. Neurophysiol.* **79**, 1902 (1998).
- [7] W. Rall, in *Handbook of Physiology*, edited by E. R. Kandel (American Physiological Society, 1977), vol. 1, pp. 39–98.
- [8] R. C. Coelho and L. da F. Costa, in *IEEE int. conf on engineering of complex systems* (1997), pp. 223–8.
- [9] G. A. Ascoli, *Network: Comput. Neural Syst.* **13**, 247 (2002).
- [10] G. Ascoli, in *Computational neuroanatomy: principles and methods*, edited by G. Ascoli (Humana Press, 2002), chap. 3, pp. 49–70.
- [11] E. R. Kandel and J. H. Schwartz, *Principles of Neuroscience* (Elsevier, New York, 1985).
- [12] R. M. Cesar and L. da F. Costa, *Rev. Sci. Instrum* **68**, 2177 (1997).
- [13] L. da F. Costa and T. J. Velte, *Journal of Comparative Neurology* **404**, 33 (1999).
- [14] R. M. Cesar and L. da F. Costa, *Biological Cybernetics* **79**, 347 (1998).
- [15] L. da F. Costa, *Real-Time Imaging* **6**, 415 (2000).
- [16] A. X. Falcao, L. da F. Costa, and B. S. Cunha, *Pattern recognition* **7**, 1571 (2002).
- [17] K. Michelsen and H. de Raedt, *Physics Report* **347**, 461 (2001).
- [18] K. Michelsen and H. de Raedt, *Computer Physics Communication* **132**, 94 (2000).
- [19] K. R. Mecke, *Int. J. of Mod. Phys.* **12**, 861 (1998).
- [20] K. Morigiwa, M. Tauchi, and Y. Fukuda, *Neurosci. Res.* **10**, S131 (1989).
- [21] L. da F. Costa, E. T. M. Manoel, F. Faucreau, J. Chelly, J. van Pelt, and G. Ramakers, *Network: Comput. Neural Syst.* **13**, 283 (2002).
- [22] L. da F. Costa, E. T. M. Manoel, and A. G. Campos, *An integrated approach to shape analysis: results and perspectives* (Cépaduès-Éditions, 2001), vol. T1, pp. 23–34.

- [23] L. A. Santaló, *Integral Geometry and Geometric Probability* (Addison-Wesley,, Reading, Ma, 1976).
- [24] L. da F. Costa and E. T. M. Manoel, *Optical Engineering* **40**, 1752 (2001).
- [25] A. Mizrahi, E. Ben-Ner, M. J. Katz, K. Kenden, J. G. Glusman, and F. Libersat, *Journal of comparative neurology* **422(3)**, 415 (2000).